European Journal of Medicinal Chemistry 44 (2009) 1870–1877

Contents lists available at ScienceDirect

European Journal of Medicinal Chemistry

journal homepage: http://www.elsevier.com/locate/ejmech

Original article

Gallium(III) complexes of 2-pyridineformamide thiosemicarbazones: Cytotoxic activity against malignant glioblastoma

Isolda C. Mendes [a], Marcela A. Soares [b], Raquel G. dos Santos [b], Carlos Pinheiro [c], Heloisa Beraldo [a,*]

[a] Departamento de Química, Universidade Federal de Minas Gerais, 31270-901 Belo Horizonte, MG, Brazil
[b] Centro de Desenvolvimento da Tecnologia Nuclear, CDTN, 31270-901 Belo Horizonte, MG, Brazil
[c] Departamento de Física, Universidade Federal de Minas Gerais, 31270-901 Belo Horizonte, MG, Brazil

ARTICLE INFO

Article history:
Received 26 August 2008
Received in revised form
28 October 2008
Accepted 4 November 2008
Available online 19 November 2008

Keywords:
Thiosemicarbazones
Gallium complexes
Glioblastoma
Cytotoxicity

ABSTRACT

The gallium(III) complexes $[Ga(2Am4DH)_2]NO_3$ (**1**), $[Ga(2Am4Me)_2]NO_3$ (**2**) and $[Ga(2Am4Et)_2]NO_3$ (**3**) were prepared with 2-pyridineformamide thiosemicarbazone (H2Am4DH) and its *N*(4)-methyl (H2Am4Me) and *N*(4)-ethyl (H2Am4Et) derivatives. The thiosemicarbazones were cytotoxic against malignant RT2 glioblastoma cells (expressing p53 protein) with IC_{50} values in the 7.3–360 μM range, and against malignant T98 glioblastoma cells (expressing mutant p53 protein) with IC_{50} values in the 3.6–143 μM range. Coordination to gallium strongly increased the cytotoxic potential in complexes **2** and **3**, which showed IC_{50} values in the 0.81–9.57 μM range against RT2 cells and in the 3.6–11.30 μM range against T98 cells, and were 20-fold more potent than cisplatin. All thiosemicarbazones and gallium complexes were able to induce cell death by apoptosis.

© 2008 Elsevier Masson SAS. All rights reserved.

1. Introduction

α(*N*)-Heterocyclic thiosemicarbazones and their metal complexes have been extensively investigated as potential antitumor agents [1]. This search for an effective anticancer agent led to the onset of clinical studies of 3-aminopyridine-2-carboxaldehyde thiosemicarbazone (3-AP; Triapine) [2,3]. It has been demonstrated that the mechanism of action of these compounds involves inhibition of the iron-dependent enzyme ribonucleoside diphosphate reductase, RDR, which catalyzes the conversion of ribonucleotides into deoxyribonucleotides during DNA syntheses [2–5].

Gallium has shown efficacy in the treatment of accelerated bone resorption, autoimmune diseases, infection and cancer [5]. The cytotoxicity of gallium is, in part, due to inhibition of transferrin receptor-mediated iron uptake by cells and perturbation of cellular iron-dependent processes, including deoxyribonucleotide syntheses [6]. Gallium activity against tumors is thought to be due to its antiproliferative and antimitotic effects. Once gallium gets into the cell it exerts its antiproliferative effects by inhibiting RDR. Due to the competitive binding of gallium(III) and iron(III), gallium affects intracellular iron availability, but it also interacts directly with RDR, displacing iron from the enzyme [6,7]. Tumor cells are more sensitive to the cytotoxic effects of RDR inhibition than normal cells because of the increased need of dNTPs for proliferation, and decreased adaptability and low responsiveness to regulatory signals. Thus, the enzyme has long been considered an excellent target for cancer chemotherapy.

Gallium is the second metal, after platinum to be used in cancer treatment [8]. Clinical trials have shown particular efficacy of gallium against bladder and urothelial carcinomas and some lymphomas [5]. Gallium salts are taken up more efficiently and more specifically by tumor cells when orally administered [6,8]. Gallium nitrate has been approved for the treatment of hypercalcemia of malignancy but its unfavorable pharmacokinetics has prevented its widespread use in systemic chemotherapy of cancer. Parenteral administration is associated with a low therapeutic index due to renal toxicity [6,8]. Therefore, the preparation of gallium(III) complexes with tumor-inhibiting properties could be a strategy to circumvent these problems.

Indeed, coordination of gallium with organic ligands has been recognized as a promising strategy for creating tumor-inhibiting therapeutic agents with a number of advantages over gallium salts regarding oral bioavailability, hydrolytic stability and membrane penetration ability [9].

Gallium(III) complexes with thiosemicarbazones containing the metal and ligand to be directed to the same molecular target could in principle present attractive pharmacological properties [6]. Our group recently started a study of the pharmacological profile of 2-pyridineformamide-derived thiosemicarbazones and their metal complexes [10,11]. As part of this investigation gallium(III)

* Corresponding author. Tel.: +55 31 3499 5740; fax: +55 31 3499 5700.
E-mail address: hberaldo@ufmg.br (H. Beraldo).

0223-5234/$ – see front matter © 2008 Elsevier Masson SAS. All rights reserved.
doi:10.1016/j.ejmech.2008.11.006

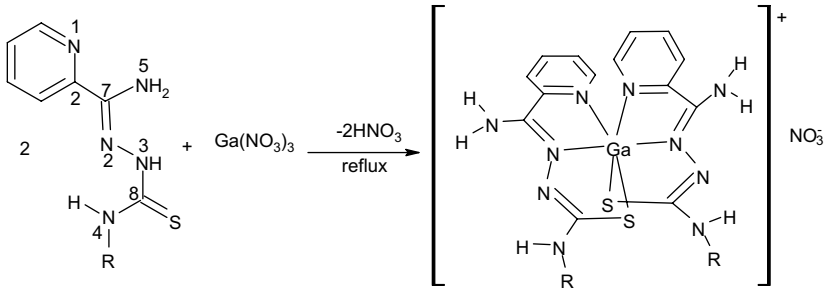

Fig. 1. Complexation reaction of 2-pyridineformamide-derived thiosemicarbazones (R = H, H2Am4DH; R = methyl, H2Am4Me; R = ethyl, H2Am4Et) with gallium nitrate.

complexes of 2-pyridineformamide thiosemicarbazone (H2Am4DH) and its *N*(4)-methyl (H2Am4Me) and *N*(4)-ethyl (H2Am4Et) derivatives (Fig. 1) were prepared and assayed for their cytotoxic activity against malignant glioblastoma cells.

2. Results and discussion

2.1. Formation of the gallium(III) complexes

Microanalyses and molar conductivity data are compatible with the formation of $[Ga(2Am4DH)_2]NO_3$ (**1**), $[Ga(2Am4Me)_2]NO_3$ (**2**) and $[Ga(2Am4Et)_2]NO_3$ (**3**), in which two anionic thiosemicarbazones are attached to the metal centre and a nitrate acts as counter-ion. Upon slow diffusion of complex **3** in 1:9 DMSO:acetone crystals of $[Ga(2Am4Et)_2]NO_3 \cdot DMSO$ were formed.

2.2. Spectroscopic characterization

The vibrations attributed to ν(C=N) at 1663–1660 cm^{-1} in the infrared spectra of the thiosemicarbazones shift to 1652–1648 cm^{-1} in the spectra of complexes **1**–**3**, in agreement with coordination of the azomethine nitrogen [10–14]. The ν(CS) absorption observed in the 855–847 cm^{-1} range in the spectra of the free thiosemicarbazones shifts to 756–746 cm^{-1} in the spectra of complexes **1**–**3**, indicating coordination of the sulfur. The 100 cm^{-1} shift is compatible with complexation of a thiolate sulfur [10,11]. The in-plane deformation mode of the pyridine ring at 622–600 cm^{-1} in the spectra of the uncomplexed thiosemicarbazones shifts to 652–642 cm^{-1} in complexes **1**–**3**, suggesting coordination of the hetero-aromatic nitrogen [10,11].

In the spectra of complexes **1**–**3** the absorptions at 433–412 cm^{-1} and 347–326 cm^{-1} were attributed to the ν(Ga–S) and ν(Ga–N) (imine) vibrations and those at 240–205 cm^{-1} to $\nu(Ga–N_{py})$ vibrations [6]. Therefore, in the complexes the thiosemicarbazones are attached to the metal through the N_{py}–N–S chelating system. Absorptions at 1450–1300 cm^{-1} were attributed to the nitrate group as counter-ion in the spectra of all complexes [15].

The NMR spectra of the thiosemicarbazones and their gallium(III) complexes were recorded in DMSO-d_6 because this is the only solvent which dissolves all ligands and complexes. The ^1H resonances were assigned on the basis of chemical shifts and multiplicities. The carbon type (C, CH) was determined by using distortionless enhancement by polarization transfer (DEPT 135) experiments. The assignments of the protonated carbons were made by 2D hetero-nuclear multiple quantum coherence experiments (HMQC).

The N3–H chemical shifts in the spectra of the thiosemicarbazones occur at δ 10.07–9.99 ppm, indicating hydrogen bonding with the solvent [10,16]. This signal is absent in the spectra of **1**–**3**, according to deprotonation and formation of an anionic ligand. Upon coordination the signals of the pyridine hydrogens as well as those of N4–H and N5–H undergo significant shifts, according to coordination of the imine nitrogen attached to C7 and of the sulfur attached to C8 [10]. Variations also occur in the ^{13}C NMR spectrum for the signals of C7, C8 and the pyridine carbons, in accordance with coordination of the sulfur, the imine nitrogen and the hetero-aromatic nitrogen, leading to compounds in which the thiosemicarbazone adopts the *EZ* configuration in relation to the C7–N2 and N3–C8 bonds [10,16–18].

2.3. X-ray diffraction analysis

Fig. 2 is a perspective view of $[Ga(2Am4Et)_2](NO_3) \cdot DMSO$. The disordered salvation DMSO molecule was not included. Selected intra-molecular bond distances and angles in the complex are given in Table 1. The distances and angles observed for the two thiosemicarbazone ligands are very similar (see Table 1). The crystal structure of H2Am4Et has been previously determined by other authors [14].

The gallium atom is coordinated by two tridentate ligands in a distorted octahedral enviroment. The N202–Ga–N102, N201–Ga–S201 and N101–Ga–S101 angles, 166.35(6)°, 159.02(4)° and 157.16(5)°, deviate markedly from the ideal value of 180°. Distorted octahedral environments were also observed by other authors for $[Ga(L)_2]^+[GaCl_4]^-$ with 2-acetylpyridine *N*(4)-dimethylthiosemi carbazone and for $[Ga(L)_2]^+[PF_6]^-$ with acetylpyrazine *N*,*N*-dimethylthiosemicarbazone, in which the N2–Ga–N2′, N1–Ga–S1 and N1′–Ga–S1′ angles (N1′, N2′ and S1′ stand for the atoms in the second ligand molecule) were 171.18(9)°, 160.12(7)°, 158.89(7)° and 162.37(5)°, 160.02(5)° 159.75(5)°, respectively [6].

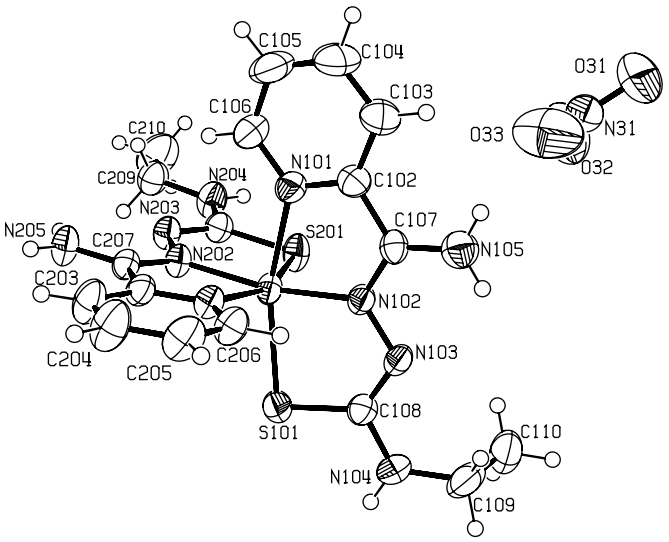

Fig. 2. Molecular plot of $[Ga(2Am4Et)]NO_3$ (**3**) showing the labeling scheme of the non-H atoms and their displacement ellipsoids at the 50% probability level. The DMSO molecule is omitted.

Table 1
Selected bond distances and angles in the crystal structure of $[Ga(2Am4Et)_2]NO_3 \cdot DMSO$.

Atoms	Distances (Å) molecules		Atoms	Angles (°) molecules		Atoms	Angles (°)
	1	2		1	2		
Ga–S01	2.380(8)	2.358(7)	C07–N02–N03	116.0(2)	116.0(2)	N202–Ga–S101	108.52(5)
Ga–N01	2.200(2)	2.171(2)	C08–N03–N02	113.1(2)	113.1(2)	N202–Ga–N101	91.36(7)
Ga–N02	1.999(2)	1.997(2)	N03–C08–N04	117.7(2)	117.0(2)	N202–Ga–N102	166.35(6)
S01–C08	1.753(2)	1.756(2)	N03–C08–S01	126.5(1)	126.5(2)	N201–Ga-N101	83.48(6)
N02–C07	1.307(3)	1.307(3)	N04–C08–S01	115.8(2)	116.5(2)	S201–Ga–S101	102.17(2)
N02–N03	1.399(2)	1.390(2)	C08–N04–C09	122.8(2)	121.9(2)	S201–Ga–N102	101.94(5)
N03–C08	1.315(2)	1.316(2)	N02–C07–N05	123.6(2)	123.5(2)	N201–Ga–N102	96.33(6)
N04–C08	1.362(2)	1.353(2)	N01–Ga–S01	157.16(5)	159.02(4)	S201–Ga–N101	90.92(5)
N04–C09	1.457(3)	1.447(3)	N02–Ga–S01	82.84(5)	83.41(5)	N201–Ga–S101	90.18(4)
N05–C07	1.332(2)	1.326(2)	N02–Ga–N01	76.12(6)	76.56(6)	–	–

* S01 stands for S101 or S201; N01 stands for N101 or N102, etc for molecules 1 and 2, respectively.

Table 2
Hydrogen bonds distances [Å] and angles [°] for $[Ga(2Am4Et)_2]NO_3 \cdot DMSO$ (H···A < r(A) + 2.00 and ⟨DHA⟩110°).

D–H···A	d(D–H)	d(H···A)	⟨DHA⟩	d(D···A)
N105–H15A···O40	0.860	2.28	140.9	2.997(3)
N105–H15B···O32	0.860	2.31	141.2	3.027(4)
N105–H15B···O33	0.860	2.38	159.4	3.201(4)
N204–H24A···O32 [x, $-y+3/2$, $z+1/2$]	0.860	2.34	151.4	3.124(4)
N205–H25B···O40 [$-x+1$, $y+1/2$, $-z+3/2$]	0.860	2.09	162.5	2.924(3)

Symmetry transformations used to generate equivalent atoms in brackets.

A twisting of approximately 180° in the N3–C8 bond of the thiosemicarbazone to match the steric requirements of tridentate coordination was evidenced. Therefore, in the complex the ligand adopts the *EZ* conformation. Hence some angles undergo significant changes on complexation. The C8–N3–N2 angle goes from 117.5° in H2Am4Et to 113.1(2)° in **3**; N3–C8–S1 goes from 119.8° in H2Am4Et to 126.5(2)° in **3**; N4–C8–S1 varies from 123.9° in H2Am4Et to 115.8(2)° and 116.5(2)° in **3**. In one of the ligands the thiosemicarbazone chain and the *N*(4)-ethyl group are practically

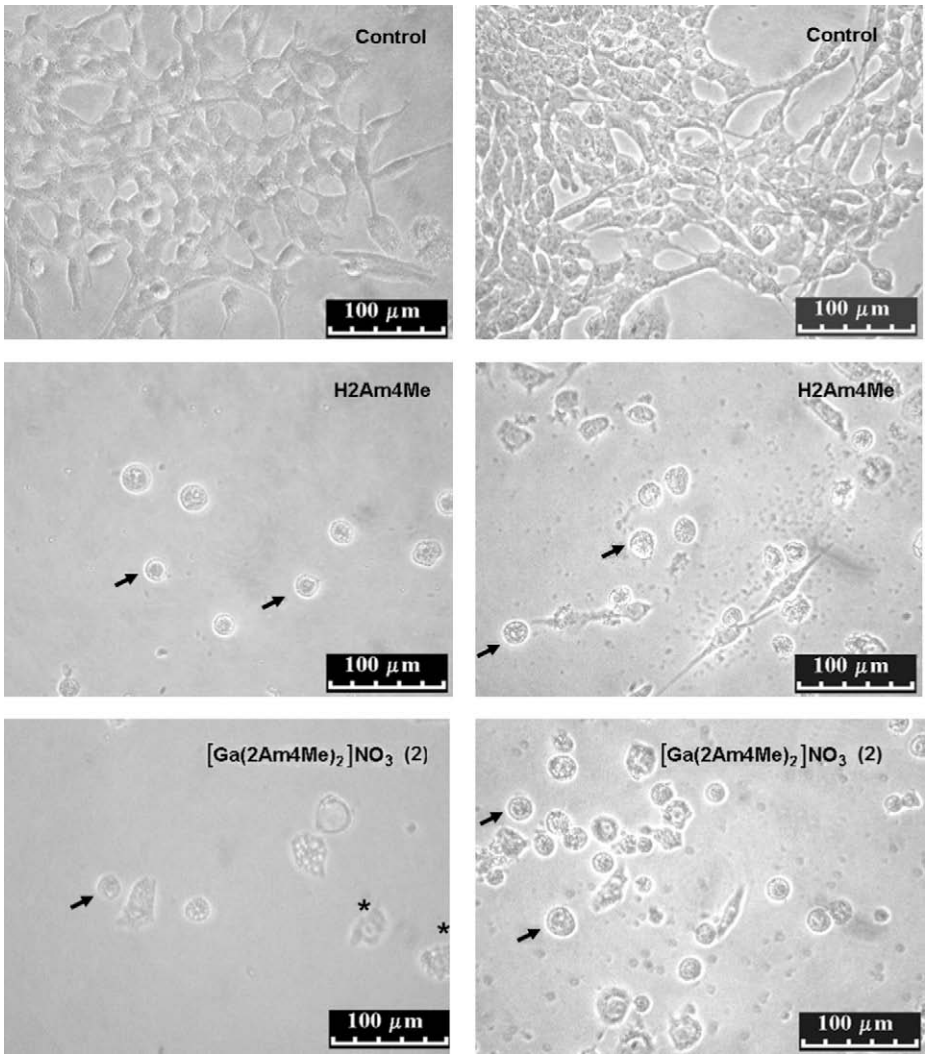

Fig. 3. Cells treated with thiosemicarbazones (10^{-4} M) exhibit membrane changes characteristic of apoptosis. Control or treated RT2 (on the left column) and T98 (on the right column) cells were incubated in culture dishes. After 48 h treatment the dishes were observed under phase contrast and membrane morphology photographed. Characteristics of apoptosis are clearly visible and are indicated: retraction of cell expansions, rounding cell (arrows), blebs (*). Magnification ×200.

in the same plane while in the other the angle between the *N*(4)-ethyl group and the thiosemicarbazone chain is 82.4(1)°.

There is a slight shortening of the bond distance between gallium and the imine nitrogen (1.999(2) and 1.997(2) Å) compared to the distance between gallium and the hetero-aromatic nitrogen (2.200(2) and 2.171(2) Å). Similar feature was observed in the gallium complex with 2-acetylpyridine *N*(4)-dimethylthiosemicarbazone, with Ga–N_{imine} bond distances (2.033(2) and 2.038(2) Å) longer than Ga–N_{py} bond distances (2.131(2) and 2.114(2) Å). By contrast, in the case of the complex with acetylpyrazine *N*,*N*-dimethylthiosemicarbazone the Ga–N_{py} bond distances (2.036(2) and 2.037(2) Å) are smaller than the Ga–N_{imine} bond distances (2.141(2) and 2.164(2) Å) [6].

The expected lengthening of the C8–S1 bonds from 1.697 Å in H2Am4Et [14] to 1.756(2) and 1.753(2) Å in **3**, and shortening of the N3–C8 bonds, from 1.354 Å in H2Am4Et [14] to 1.316(2) and 1.315(2) Å in **3** were observed. Therefore, the C8–S1 bond changes from a double to a predominantly single bond whereas N3–C8 acquires some double bond character.

In the packing of $[Ga(2Am4Et)_2]NO_3 \cdot DMSO$ a number of intermolecular hydrogen bonds occur involving N204–H, N105–H and the oxygen atoms of the nitrate anion; hydrogen bonds involving N105–H, N205–H and the oxygen from DMSO were evidenced as well (see Table 2).

2.4. Cytotoxic activity against malignant RT2 and T98 glioblastoma cells

2.4.1. Thiosemicarbazones and their gallium(III) complexes induce membrane changes characteristics of apoptosis

A wide range of phenotypic modifications occurred in glioblastoma cells after exposure to the thiosemicarbazones and their gallium(III) complexes. Fig. 3 shows, as examples, control glioblastoma cells and cells treated with H2Am4Me and with complex **2**. After treatment with all thiosemicarbazones and gallium complexes, retraction of the cytoplasmatic expansions, leading to round shaped cells, cell shrinkage and blebs formation were noticed. Reduction of the number of cells after treatment was also observed. These morphological changes are associated with apoptosis.

2.4.2. Thiosemicarbazones and their gallium(III) complexes induce nuclear changes characteristics of apoptosis

Triggering of programmed cell death (apoptosis) induces DNA fragmentation through the activation of specific DNA endonucleases [19]. Activation of nucleases can be evidenced through the use of DNA staining with 4′,6′-diamidino-2-phenylindole (DAPI), which detects fragmented and condensed DNA. No DNA fragmentation was observed in the untreated cells, but following exposure to the

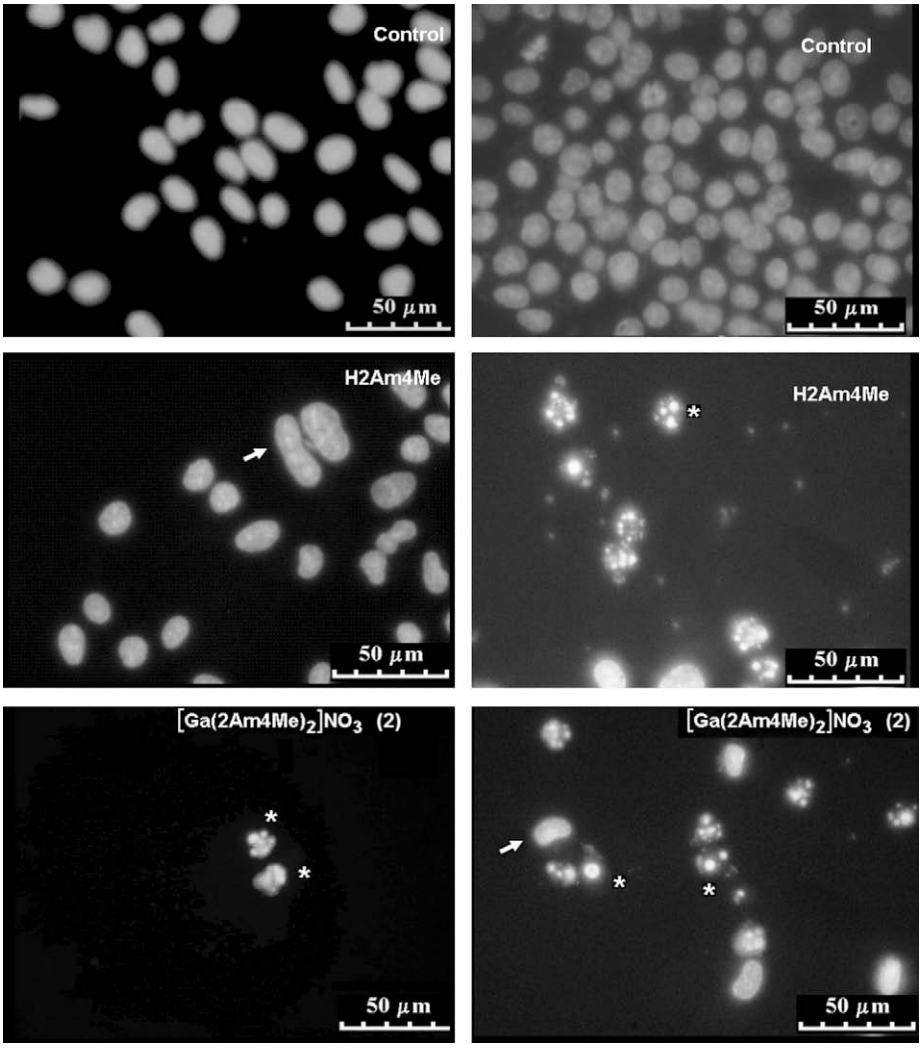

Fig. 4. Cells treated with thiosemicarbazones exhibit nuclear changes characteristic of apoptosis. RT2 (on the left column) and T98 (on the right column) cells were treated with thiosemicarbazones (10^{-4} M) or diluent (Control). After 48 h treatment, cells were fixed and stained with DAPI as described in Section 4.8. It can be observed chromatin condensation, nuclear fragmentation (arrows) and apoptotic bodies (*). Magnification ×400.

Table 3
Cytotoxic effect of 2-pyridineformamide-derived thiosemicarbazones and their gallium (III) complexes on glioblastoma cells.

Compound	IC_{50}	
	RT2	T98
Cisplatin	17 ± 1	5 ± 3
H2Am4DH	7.28 ± 0.09	3.6 ± 0.3
H2Am4Me	12.2 ± 0.7	32 ± 1
H2Am4Et	359 ± 10	143 ± 41
$[Ga(2Am4DH)_2]NO_3$ (**1**)	5.31 ± 0.03	5.7 ± 0.3
$[Ga(2Am4Me)_2]NO_3$ (**2**)	0.81 ± 0.03	4.7 ± 0.9
$[Ga(2Am4Et)_2]NO_3$ (**3**)	9.6 ± 0.6	4.0 ± 0.8
$Ga(NO_3)_3$	>100	>1000

thiosemicarbazones and their gallium(III) complexes, cells exhibited extensive DNA fragmentation as seen in Fig. 4 for H2Am4Me and complex **2**.

2.4.3. Glioblastoma cytotoxicity

The concentrations of the studied compounds which kill 50% of RT2 and T98 glioblastoma cells (IC_{50}) are listed in Table 3. The concentration–effect curves for the thiosemicarbazones and complexes **1**–**3** are shown in Fig. 5. All thiosemicarbazones as well as their gallium complexes were highly active against malignant glioblastoma. H2Am4DH, $IC_{50} = 7.3$ μM (RT2) and $IC_{50} = 3.6$ μM (T98) and H2Am4Me, $IC_{50} = 12.2$ μM (RT2) and $IC_{50} = 32$ μM (T98) were as active as the antitumor agent cisplatin, $IC_{50} = 17$ μM (RT2) and $IC_{50} = 5$ μM (T98), while H2Am4Et, $IC_{50} = 359$ μM (RT2) and $IC_{50} = 143$ μM (T98) showed a much lower cytotoxic activity. The activity decreases in the series H2Am4DH > H2Am4Me > H2Am4Et probably because increasing the bulkiness of the *N*4-substituent does not facilitate the interaction of the thiosemicarbazone with the biological targets. Interestingly, H2Am4DH and H2Am4Et were twice more active against T98 cells.

On the other hand, it is worth noting that coordination to gallium strongly increased the cytotoxic potential of the *N*(4)-methyl (H2Am4Me) and *N*(4)-ethyl (H2Am4Et) substituted thiosemicarbazones (see Table 3) generating compounds up to 20-fold more potent than cisplatin. The cytotoxicities of $Ga(NO_3)_3$, $IC_{50} > 100$ μM (RT2) and $IC_{50} > 1000$ μM (T98), were lower than those of all studied compounds. In all cases upon coordination to the thiosemicarbazone, gallium lipophilicity probably increases. Since neither gallium nitrate nor H2Am4Et presented as good cytotoxic activity as the other studied compounds, the high cytotoxic effect of **3** is probably due to the complex as an entity.

As shown by crystal structure determinations all thiosemicarbazones adopt the *EE* conformation in the solid [12–14]. Weak intra-molecular N4–H···N2 hydrogen bonds are present, which probably do not facilitate rotation around N3–C8 in solution, specially for the bulkier *N*(4)-methyl and *N*(4)-ethyl derivatives, which are less active than the unsubstituted thiosemicarbazone. By increasing the bulkiness of the *N*(4)-substituent, conversion from the *EE* to the *EZ* conformation is probably hampered. Considering that upon coordination all thiosemicarbazones adopt the *EZ* configuration and that activity increases, the *EZ* form is probably more suitable for the interaction with the biological targets. In fact the enhancement of activity upon coordination is more pronounced in the case of the bulkiest *N*(4)-ethyl derivative.

Other groups reported the cytotoxicity of gallium(III) complexes with acetylpyridine and acetylpyrazine-derived *N*-heterocyclic thiosemicarbazones against the 41 M (ovarian carcinoma), SK-BR-3 (mammary carcinoma) and SW480 (colon carcinoma) human cancer cell lines, with IC_{50} values in the nanomolar range [6]. However, to our knowledge the present work reports for the first time the cytotoxicity of gallium complexes against brain tumor cells.

2.4.4. Hematotoxicity

The release of hemoglobin was used to quantify the membrane-damaging properties of the compounds. The hemolysis test evaluated the red blood cells (RBCs) membrane disruption potential of the studied compounds. This assay uses the RBC membrane as an endosomal membrane model [20]. Under the assayed conditions, the hemolytic activity of gallium nitrate and all studied compounds was very low at pH 7.4 ($IC_{50} > 10^{-3}$ M), near that of the control sample, indicating no detectable disturbance of red blood cell membrane.

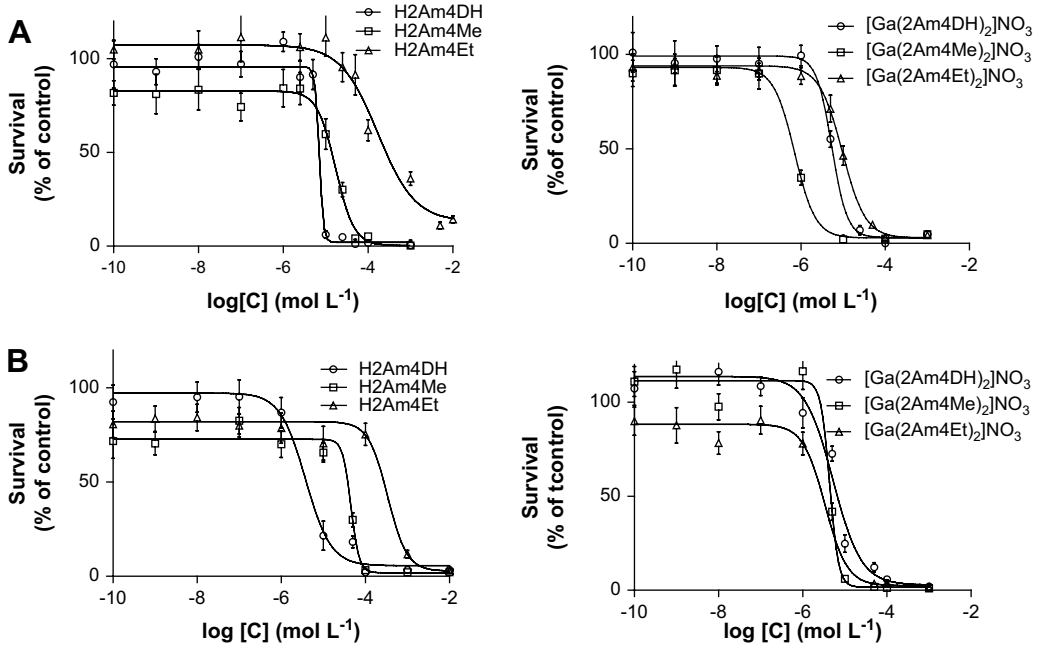

Fig. 5. Concentration–effect curves for the thiosemicarbazones and complexes **1**–**3** obtained by the MTT assay in RT2 (A) and T98 (B) gliobalstom cells.

3. Conclusions

It is well known that glioblastoma cells express wild-type p53 protein [21]. In fact, apoptosis of these cells is triggered primarily by a p53 pathway, evidencing that RT2 cells have functional p53 protein. Previous characterization of p53 genotype and drug sensitivity of human cancer cell lines has revealed that cells with mutant or absent p53 are less sensitive than cells with wild-type p53 to the majority of clinically used anticancer agents, including DNA alkylating agents.

H2Am4DH and H2Am4Et were more active against T98 (with mutant p53) cells while H2Am4Me was more cytotoxic against RT2 (presenting wild-type p53) cells. Complexes **1** and **3** showed similar cytotoxic activities against both cell lines while complex **2** showed higher activity against RT2 cells. Therefore, the thiosemicarbazones and their gallium(III) complexes can probably activate apoptotic cell death pathways by mechanisms that are both dependent and independent of p53. Hence the studied compounds can recruit more than one pathway to trigger cell death, therefore, enhancing their utility in anticancer therapy.

Upon coordination the cytotoxic activity of H2Am4Me and H2Am4Et increased against not only wild-type p53-expressing but also against p53-mutant cells. The glioblastoma cells used in this work were resistant to gallium nitrate, $IC_{50} > 10^{-4}$ M (RT2); $IC_{50} > 10^{-3}$ M (T98). Therefore, coordination leads to the enhancement of the cytotoxic effect of the thiosemicarbazones and of gallium. Considering that glially differentiated neoplasms (glioblastoma) proved to be less sensitive than the primitive, poorly differentiated medulloblastoma and rhabdomyosarcoma tumors to DNA synthesis inhibition by gallium nitrate [22], the abovementioned results indicate that coordination of gallium to thiosemicarbazones could be a strategy of broadening the spectrum of antitumor activity of both gallium and thiosemicarbazones against brain tumors.

Because approximately two-thirds of gliomas have defects in the p53 pathway, the ability of the studied compounds to affect cells regardless of their p53 status suggests that they have a good potential to be developed into novel drug candidates for the therapy of brain tumors. The low hemolytic activity of all studied compounds suggests that further investigations on their pharmacological behavior should be carried out.

4. Experimental

4.1. Chemicals

2-Cyanopyridine, thiosemicarbazide, *N*(4)-methylthiosemicarbazide and *N*(4)-ethylthiosemicarbazide were purchased from Aldrich and used as-received. 2-Pyridineformamide thiosemicarbazones were prepared as previously described [10–14].

4.2. Synthesis of $[Ga(2Am4DH)_2]NO_3$ (**1**), $[Ga(2Am4Me)_2]NO_3$ (**2**), $[Ga(2Am4Et)_2]NO_3$ (**3**)

The gallium(III) complexes were obtained by mixing equimolar amounts (3 mmol) of the desired ligand with gallium nitrate in ethanol under reflux during 3 h. The resulting solids were filtered and washed with ethanol and ether and dried *in vacuo*.

4.2.1. Bis(2-pyridineformamidethiosemicarbazonato)gallium(III) $[Ga(2Am4DH)_2]NO_3$ (**1**)

Orange solid; Anal. Calcd ($C_{14}H_{16}GaN_{11}O_3S_2$): C, 32.32; H, 3.10; N, 29.62. Found: C, 31.96; H, 3.18; N, 29.52%; FW: 520.20 g mol^{-1}. IR (CsI/nujol, cm^{-1}): ν(NH) 3457, ν(C=N) 1651, $\nu(NO_3)$ 1408–1303, ν(C=S) 746, ρ(py) 652, ν(GaN) 424, ν(GaS) 335,326, $\nu(Ga–N_{py})$ 240, 231 and 225. Molar conductivity (1×10^{-3} mol L^{-1} dimethylformamide, DMF): 68 Ω^{-1} cm^2 mol^{-1}. ^{1}H NMR (DMSO-d_6): δ (ppm) = 7.90 (1H, d, H(6)), 7.73 (1H, t, H(5)), 8.28 (1H, t, H(4)), 8.45 (1H, d, H(3)), 6.40 (2H, s, N(4)H), 8.07 (2H, br, N(5)H). ^{13}C NMR (DMSO-d_6): δ (ppm) = 168.99 C8, 141.13 C7, 144.23 C6, 127.93 C5, 141.91 C4, 121.72 C3, 145.09 C2. Yield 78%.

4.2.2. Bis(N(4)-methyl 2-pyridineformamide thiosemicarbazonato)gallium(III) $[Ga(2Am4Me)_2](NO_3)$ (**2**)

Orange solid; Anal. Calcd ($C_{16}H_{20}GaN_{11}O_3S_2$): C, 35.05; H, 3.68; N, 28.10. Found: C, 34.94; H, 4.01; N, 27.77%; FW: 548.25 g mol^{-1}. IR (CsI/nujol, cm^{-1}): ν(NH) 3412, ν(C=N) 1648, $\nu(NO_3)$ 1339–1301, ν(C=S) 756, ρ(py) 649, ν(GaN) 433, ν(GaS) 346, $\nu(GaN_{py})$ 227 and 213 and 205. Molar conductivity (1×10^{-3} mol L^{-1} dimethylformamide, DMF): 85 Ω^{-1} cm^2 mol^{-1}. ^{1}H NMR (DMSO-d_6): δ (ppm) = 7.87 (1H, d, H(6)), 7.72 (1H, t, H(5)), 8.28 (1H, t, H(4)), 8.47 (1H, d, H(3)), 7.06 (1H, d, N(4)H), 8.15 (2H, br, N(5)H), 2.92 (1H, d, H(9)). ^{1}C NMR (DMSO-d_6): δ (ppm) = 167.69 C8, 141.18 C7, 144.20 C6, 127.91 C5, 141.83 C4, 121.66 C3, 145.35 C2, 29.24 C9. Yield 73%.

4.2.3. Bis(N(4)-ethyl 2-pyridineformamide thiosemicarbazonate)gallium(III) $[Ga(2Am4Et)_2]NO_3$ (**3**)

Orange solid; Anal. Calcd ($C_{18}H_{24}GaN_{11}O_3S_2$): C, 37.51; H, 4.20; N, 26.73. Found: C, 37.09; H, 4.15; N, 26.59%; FW: 576.31 g mol^{-1}. IR (CsI/nujol, cm^{-1}): ν(NH) 3407, ν(C=N) 1652, $\nu(NO_3)$ 1414–1347, ν(C=S) 750, ρ(py) 642, ν(GaN) 412, ν(GaS) 347 and 336, $\nu(Ga–N_{py})$ 231, 226 and 221. Molar conductivity (1×10^{-3} mol L^{-1} dimethylformamide, DMF): 69 Ω^{-1} cm^2 mol^{-1}. ^{1}H NMR (DMSO-d_6): δ (ppm) = 7.86 (1H, d, H(6)), 7.71 (1H, t, H(5)), 8.27 (1H, t, H(4)), 8.45 (1H, d, H(3)), 7.02 (2H, s, N(4)H), 8.08 (2H, br, N(5)H), 3.47 (2H, m, H(9)), 1.14 (3H, t, H(10)). ^{13}C NMR (DMSO-d_6): δ (ppm) = 166.87 C8, 141.12 C7, 144.02 C6, 127.72 C5, 141.68 C4, 121.49 C3, 145.09 C2, 36.77 C9, 14.34 C10. Yield 76%.

4.3. Physical measurements

Partial elemental analyses were performed on a Perkin Elmer CHN 2400 analyzer. Infrared spectra were recorded on a Perkin Elmer FT-IR Spectrum GX spectrometer using CsI pellets; an YSI model 31 conductivity bridge was employed for molar conductivity measurements; NMR spectra were obtained at room temperature with a Brucker DRX-400 Avance (400 MHz) spectrometer using deuterated dimethyl sulfoxide (DMSO-d_6) as the solvent and tetramethylsilane (TMS) as internal reference. Splitting patterns are designated as follows; s, singlet; d, doublet; t, triplet; q, quartet; m, multiplet.

4.4. Crystal structure

Suitable crystals for X-ray diffraction of $[Ga(2Am4Et)_2]NO_3 \cdot$DMSO were obtained from slow evaporation of a 1:9 DMSO/acetone solution and mounted on a glass fiber. Data were collected at room temperature on a Bruker-Kappa-CCD diffractometer using graphite-monochromatized Mo Kα radiation ($\lambda = 0.71073$ Å). Final unit cell parameters were based on the fitting of all reflections positions (DIRAX9) [23]. Data integration and scaling of the reflections were performed with the EVALCCD suite [24]. The structure was solved by direct methods and refined on F^2 by full-matrix least-squares using the SHELX-97 [25,26] program in a WinGX system [27]. Crystal data, data collection procedure, structure determination methods and refinement results are summarized in Table 4.

Although some of the hydrogen atoms could be identified in a Fourier difference map, in the final model they were geometrically positioned and refined using a riding model. All non-H atoms were refined anisotropically. Molecular graphics was obtained from ORTEP [28].

Table 4
Crystal data and structure refinement for $[Ga(2Am4Et)_2]NO_3 \cdot DMSO$.

Empirical formula	C20 H30 N11 O4 S3 Ga
Crystal size (mm)	$0.25 \times 0.19 \times 0.13$
Molecular weight ($g\,mol^{-1}$)	654.45
Cristal system, space group	Monoclinic $P2(1)/c$
Lattice parameters	
a (Å)	8.730(2)
b (Å)	17.919(4)
c (Å)	18.884(4)
β (°)	100.72(3)
V (Å^3)	2902.5(10)
Z	4
$F(000)$	1352
D_{calc} ($g\,cm^{-3}$)	1.498
Absorption coefficient (mm^{-1})	1.211
θ Range for data collection (°)	5.12 to 26.37
Limiting indices	$-10 \le h \le 10$, $-22 \le k \le 22$, $-23 \le l \le 23$
Reflections collected	70,647
Reflections unique/R(int)	5875/0.0605
Reflections [$I > 2\sigma(I)$]	4620
Completeness to $\theta = 26.37$	99.2%
Parameters/restraints	362/0
Final R indices [$I > 2\sigma(I)$]	$R1 = 0.0321$, $wR2 = 0.0841$
R indices (all data)	$R1 = 0.0455$, $wR2 = 0.0896$
Goodness-of-fit on F^2	1.054
Largest diff. peak and hole (e Å^{-3})	0.938/−0.387

4.5. Cell lines and culture conditions

Malignant RT2 (wild-type) and T98 (mutant p53) glioblastoma cells were maintained in Dulbecco's Modified Eagle's Medium (DMEM-Gibco), supplemented with 10% fetal bovine serum and antibiotics (50 U mL^{-1} penicillin/50 μM streptomycin), in a water-jacketed incubator with humidified atmosphere of 5% CO_2/95% air at 37 °C. For all experiments, cells were seeded at appropriate concentrations to ensure exponential growth.

4.6. Cytotoxic activity

To determine the IC_{50} values the cytotoxic effects were quantified using a 3-(4,5-dimethiol-2-thioazolyl)-2,5-diphenyl tetrazolium bromide (MTT) colorimetric assay [29]. Briefly, logarithmic phase glioblastoma cells were treated with increasing concentrations of cisplatin (positive control) and test compounds (1×10^{-12} M to 1×10^{-2} M). Drugs were previously dissolved in dimethyl sulfoxide (DMSO) and the final concentrations were adjusted in DMEM in such manner that final DMSO concentration was lower than 0.5%. Following 48 h treatment, MTT reagent was added to each well. Following another 4 h of incubation at 37 °C, DMSO was added to each well to dissolve formazan precipitates and absorbance was measured at 570 nm. Tests using DMSO (0.5% in DMEM) as negative control were carried out in parallel.

4.7. Statistical analysis

Data were reported as mean + SD, expressed as percentage of cell viability relative to the untreated control. All tests were performed in triplicates with full agreement between the results. The statistical significance was assessed using Student's t-test ($p < 0.05$).

4.8. Morphological analysis of tumor cells

For phase contrast microscopy, representative fields of cells were photographed using a TS100 (Nikon) microscope. Cells stained with DAPI were visualized using suspensions of treated or control cells placed in tissue culture dishes. Cells were fixed with methanol, rinsed with PBS and methanol, stained with DAPI in methanol, and observed using fluorescence microscopy (Nikon) under UV illumination.

4.9. Direct hemolysis assay

The hemolytic activity of the studied compounds was evaluated according to Fisher et al. [30]. Human blood, collected in tubes containing EDTA, was centrifuged at 700 g for 10 min. The pellet was washed three times with cold PBS pH 7.4 by centrifugation, and resuspended in the same buffer. The release of hemoglobin was used to quantify the membrane-damaging properties of the compounds. As 100% and 0% values we used Triton X-100 and phosphate-buffer-treated erythrocytes, respectively. Erythrocytes were incubated with increasing concentrations of the compounds in the 10^{-8}–10^{-3} M range for 1 h at 37 °C in a shaker water bath. The release of hemoglobin was determined after centrifugation by photometric analysis at 540 nm. Complete hemolysis was achieved using Triton X-100 yielding the 100% control value. Less than 10% hemolysis was regarded as non-toxic effect level in our experiments. The experiments were run in triplicates and were repeated twice.

5. Supplementary material

CCDC reference number 699609 for $[Ga(2Am4Et)_2]NO_3 \cdot DMSO$ contains the supplementary crystallographic data. These data can be obtained free of charge from the CCDC via www.ccdc.cam.ac.uk/data_request/cif.

Acknowledgements

X-ray diffraction measurements were performed in the Laboratório de Difração de Raios X from Universidade Federal Fluminense (LDRX-UFF), Niterói, Brazil. This work was supported by Fundação de Amparo a Pesquisa do Estado de Minas Gerais (FAPEMIG), Centro de Desenvolvimento da Tecnologia Nuclear, Comissão Nacional de Energia Nuclear (PCI/CNEN), Conselho Nacional de Desenvolvimento Científico e Tecnológico (CNPq) and Instituto do Milênio-Inovação e Desenvolvimento de Novos Fármacos e Medicamentos (IM-INOFAR, Proc. CNPq 420015/05-1).

References

[1] H. Beraldo, D. Gambino, Mini-Rev. Med. Chem. 4 (2004) 31–39.
[2] R.A. Finch, M.C. Liu, S.P. Grill, W.C. Rose, R. Loomis, K.M. Vasquez, Y.C. Cheng, A.C. Sartorelli, Biochem. Pharmacol. 59 (2000) 983–991.
[3] R.A. Finch, M.C. Liu, A.H. Cory, J.G. Cory, A.C. Sartorelli, Adv. Enzyme Regul. 39 (1999) 3–12.
[4] I. Gojo, M.L. Tidwell, J. Greer, N. Takebe, K. Seiter, M.F. Pochron, B. Johnson, M. Sznol, J.E. Karp, Leuk. Res. 31 (2007) 1165–1173.
[5] L.R. Bernstein, Pharmacol. Rev. 50 (1998) 665–682.
[6] (a) C.R. Kowol, R. Berger, R. Eichinger, A. Roller, M.A. Jakupec, P.P. Schmidt, V.B. Arion, B.K. Keppler, J. Med. Chem. 50 (2007) 1254–1265;
(b) V.B. Arion, M.A. Jakupec, M. Galanski, P. Unfied, B.K. Keppler, J. Inorg. Biochem. 91 (2002) 298–305.
[7] C.R. Chitambar, Expert Opin. Investig. Drug 13 (2004) 531–541.
[8] P. Collery, B. Keppler, C. Madoulet, B. Desoize, Crit. Rev. Oncol. Hematol. 42 (2002) 283–296.
[9] A.V. Rudnev, L.S. Foteeva, C. Kowol, R. Berger, M.A. Jakupec, V.B. Arion, A.R. Timerbaev, B.K. Keppler, J. Inorg. Biochem. 100 (2006) 1819–1826.
[10] I.C. Mendes, J.P. Moreira, J.D. Ardisson, R.Gouvea dos Santos, P.R.O. da Silva, I. Garcia, A. Castiñeiras, H. Beraldo, Eur. J. Med. Chem. 43 (2008) 1454–1461.
[11] A.E. Graminha, F.S. Vilhena, A.A. Batista, S.R.W. Louro, R.L. Ziolli, L.R. Teixeira, H. Beraldo, Polyhedron 27 (2007) 547–551.
[12] A. Castineiras, I. Garcia, E. Bermejo, D.X. West, Z. Naturforsch. B: Chem. Sci. 55 (2000) 511–518.
[13] D.X. West, J.K. Swearingen, J. Valdes-Martinez, S. Hernandez-Ortega, A.K. El-Sawaf, F.V. Meurs, A. Castineiras, I. Garcia, E. Bermejo, Polyhedron 18 (1999) 2919–2929.
[14] E. Bermejo, A. Castineiras, I. Garcia-Santos, L.M. Fostiak, J.K. Swearingen, D.X. West, Z. Anorg. Allg. Chem. 631 (2005) 728–738.
[15] K. Nakamoto (Ed.), Infrared and Raman Spectra of Inorganic and Coordination Compounds, Jonh Wiley & Sons, New York, 1986, p. 257.

[16] A.P. Rebolledo, M. Vieites, D. Gambino, O.E. Piro, E.E. Castellano, C.L. Zani, E.M. Souza-Fagundes, L.R. Teixeira, A.A. Batista, H. Beraldo, J. Inorg. Biochem. 99 (2005) 698–706.
[17] A.P. Rebolledo, G.M. Lima, L.N. Gambi, N.L. Speziali, D.F. Maia, C.B. Pinheiro, J.D. Ardisson, M.E. Cortés, H. Beraldo, Appl. Organomet. Chem. 17 (2003) 945–951.
[18] A. Pérez-Rebolledo, G.M. Lima, N.L. Speziali, O.E. Piro, E.E. Castellano, J.D. Ardisson, H. Beraldo, J. Organomet. Chem. 691 (2006) 3919–3930.
[19] M. Enari, H. Sakahira, H. Yokoyama, K. Okawa, A. Iwamatsu, S. Nagata, Nature 391 (1998) 43–50.
[20] R.A. Jones, C.Y. Cheung, F.E. Black, J.K. Zia, P.S. Stayton, A.S. Hoffman, M.R. Wilson, Biochem. J. 372 (2003) 65–75.
[21] P.M. ÓConnor, J. Jackman, I. Bae, T.G. Myers, S. Fan, M. Mutoh, D.A. Scudiero, A. Monks, E.A. Sausville, J.N. Weinstein, S. Friend, A.J. Fornace Jr., K.W. Kohn, Cancer Res. 57 (1997) 4285–4300.
[22] H.T. Whelan, C. Przybylski, C.R. Chitambar, Pediatr. Neurol. 7 (1991) 352–354.
[23] A.J.M. Duisenberg, J. Appl. Crystallogr. 25 (1992) 92–96.
[24] A.J.M. Duisenberg, L.M.J. Kroon-Batenburg, A.M.M. Schreurs, J. Appl. Crystallogr. 36 (2003) 220–229.
[25] G.M. Sheldrick, SHELXS-97: Program for Solution of Crystal Structures, University of Göttingen, Göttingen, Germany, 1997.
[26] G.M. Sheldrick, SHELXL-97: Program for Crystal Structures Analysis, University of Göttingen, Göttingen, Germany, 1997.
[27] L.J. Farrugia, J. Appl. Crystallogr. 32 (1999) 837–838.
[28] L.J. Farrugia, J. Appl. Crystallogr. 30 (1997) 565.
[29] R.I. Freshney, Culture of Animal Cells: A Manual of Basic Technique, fourth ed. WileyLiss, 2000.
[30] D. Fisher, Y. Li, B. Ahlemeyer, J. Krieglstein, T. Kissel, Biomaterials 24 (2003) 1121–1131.